Non-linear frequency-dependent selection promotes long-term coexistence between bacteria species

Noémie Harmand, Valentine Federico, Thomas Hindre, Thomas Lenormand

Non-linear frequency-dependent selection promotes long-term coexistence between bacteria species

Harmand Noémie[1], Valentine Federico[1], Thomas Hindré [2], Lenormand Thomas[1 *]

1. UMR 5175 CEFE, CNRS - Université Montpellier - Université P. Valéry - EPHE, Montpellier Cedex 5, France

2. Univ. Grenoble Alpes, Centre National de la Recherche Scientifique (CNRS), Grenoble Institut National Polytechnique (INP), Techniques de l'Ingénierie Médicale et de la Complexité - Informatique, Mathématiques et Applications, Grenoble (TIMC-IMAG), F-38000 Grenoble, France

* Corresponding author

Authorship statement: study design HN, TH, TL; experiments NH, VF; writing TL, NH, TH; model and analysis NH, TL

Data accessibility: available on HAL https://hal.archives-ouvertes.fr/hal-02099952

Supplementary material: Detailed methods, appendix on the model, Sup Table S1, Fig S1, S2 available on HAL

Abstract

Negative frequency-dependent selection (NFDS) is an important mechanism for species coexistence and for the maintenance of genetic polymorphism. Long-term coexistence nevertheless requires NFDS interactions to be resilient to further evolution of the interacting species or genotypes. For closely related genotypes, NFDS interactions have been shown to be preserved through successive rounds of evolution in coexisting lineages. On the contrary, the evolution of NFDS interactions between distantly related species has received less attention. Here, we tracked the coevolution of *Escherichia coli* and *Citrobacter freundii* that initially differ in their ecological characteristics. We showed that these two bacterial species engaged in an NFDS interaction particularly resilient to further evolution: despite a very strong asymmetric rate of adaptation, their coexistence was maintained owing to an NFDS pattern where fitness increases steeply as the frequency decreases towards zero. Using a model, we showed how and why such NFDS pattern can emerge. These findings provide a robust explanation for the long-term maintenance of species at very low frequencies.

Keywords

Experimental coevolution, *Escherichia coli*, *Citrobacter freundii*, Nalidixic acid, polymorphism, negative frequency dependent selection, NFDS

Introduction

Astounding biodiversity can be observed at different scales: from locus to species, from newly emerging polymorphism to trans-specific polymorphisms maintained for millions of years (e.g. in (Devier et al. 2009; van Diepen et al. 2013). Understanding the maintenance of such diversity among species (coexistence in communities) and within species (genetic polymorphism) is a long-standing question in ecology and evolution. Various mechanisms can explain stable coexistence by a balance between selection and other forces, such as migration or mutation (listed in Débarre and Lenormand 2011). However, one of the most effective ways to maintain long-term coexistence or polymorphism is when selection itself operates in a frequency-dependent manner, favoring rare types. With such negative frequency-dependent selection (NFDS), by definition, a small frequency perturbation below (resp. above) the equilibrium frequency leads to positive (resp. negative) selection, bringing the system back to its equilibrium point and ensuring stability (Lewontin 1958; Haldane and Jayakar 1963; Ayala and Campbell 1974; Bell 2008; Felsenstein 2017). Apart from selection on alleles caused by overdominance in diploids, NFDS can emerge from a diversity of underlying ecological mechanisms (see Table S1). Demonstrating NFDS in field or in laboratory experiments requires measuring how relative fitness varies when the competing types are manipulated to be at different frequencies (we term "NFDS pattern" the relationship between the selection coefficient and the frequency). Such findings are usually taken as a strong argument in favor of long-term coexistence, as long as environmental conditions remain unchanged (e.g. in Turner et al. 1996; Gigord et al. 2001; Weeks and Hoffmann 2008; Takahashi and Kawata 2013; Healey et al. 2016). However, NFDS patterns may evolve, which may compromise coexistence, even under constant environmental conditions. For instance, when two types are maintained by NFDS, each can still independently adapt to the surrounding environmental conditions and to the presence of the other type, hence putatively disrupting NFDS interactions.

The evolution of NFDS patterns and long-term coexistence have been intensively studied particularly for interactions within species. The long-term persistence of polymorphic alleles in sexual species has been repeatedly demonstrated and can last hundreds of millions of years (Takahata and Nei 1990; Devier et al. 2009; Karasov et al. 2014; Těšický and Vinkler 2015). Many studies using experimental evolution on bacteria have demonstrated that emerging polymorphisms can arise, evolve and reach metastable equilibria (Turner et al. 1996; Rainey and Travisano 1998; Rozen and Lenski 2000; Friesen et al. 2004; Rozen et al. 2007; Blount et al. 2008, 2012; Plucain et al. 2014; Maddamsetti et al. 2015; Healey et al. 2016; Good et al. 2017). In those cases, coexistence can be disrupted as beneficial mutations accumulate in one competing lineage (Maddamsetti et al. 2015) or be maintained in the very long-term owing to successive rounds of

evolution in the two diverging ecotypes (Le Gac et al. 2012). The evolution of NFDS among divergent species has received, comparatively, much less attention. There are however reasons to expect a different regime for long-term coexistence in this case.

At first sight, the mechanism of negative frequency dependence applies equally well to alleles at a locus within a sexual species as it does to different clones in an asexual species or to different species in a community. And indeed, the basic theoretical models are virtually indistinguishable in these cases (Levin 1988; Mazancourt and Dieckmann 2004). However, there might be an important difference between these situations in terms of long-term coexistence. In a sexual species, alleles maintained polymorphic at a locus by NFDS are likely to share the same genetic background, except perhaps for the portion of the genome in the close vicinity of that locus. Hence the evolution of the NFDS pattern is expected to be limited since it will mostly occur by the occurrence of new alleles at that locus (e.g. for self-incompatibility, Castric and Vekemans 2004, or mating type loci, Billiard et al. 2011), as illustrated in Figure 1a. Polymorphic clones *de novo* emerging in an asexual species also share similar backgrounds, but, in that case, coexistence is expected to be less stable compared to the previous case, as NFDS patterns may evolve due to mutations and frequency variation at a large number of loci, in entire genomes evolving independently. However, the initial similarity of the two types will be unlikely to cause fast NFDS destabilization (Figure 1b). Divergent species engaging new NFDS interactions are expected to be the least prone to long-term coexistence since such genetically and phenotypically different types may immediately exhibit differences in their rate of adaptation to their common environment, which could quickly destabilize their coexistence (Figure 1c). Overall, because of intercept variation of the NFDS pattern, we would expect polymorphism maintained by NFDS to persist longer among alleles in a sexual species than among species, and longer between recently-diverged than anciently-diverged species.

The shape and slope of the NFDS pattern may also evolve. In the three situations mentioned above and illustrated in Figure 1a,b,c, the evolution of a steeper NFDS pattern will promote long-term coexistence as with a larger slope, larger changes in intercept are required to selectively eliminate one type (Figure 1d). Ultimately, it is the relative evolution of the intercept and slope of the NFDS pattern that will dictate long-term coexistence. While the variation in intercept may be expected to differ for the different cases mentioned above (alleles, recently-diverged, anciently-diverged species), there are no clear predictions for the slope. As for most situations of specialization, the relative availability of the different types of mutations (on intercept or slope) depends mostly on the shape of the underlying trade-offs that are difficult to predict (Lenormand 2012). Some of this variation might depend on the age of the NFDS relationship. Ancient coexistence situations are likely to involve interaction-stabilizing traits and relatively steeper NFDS slopes (as they have

been maintained for a long time) than more recent NFDS interactions. However, the current traits of coexisting species might have been shaped by multiple interactions with other functionally-related species in the past, even if the observed NFDS interaction is recent and involves new partners. In other words, the degree to which divergent species are expected to maintain long-term coexistence in an NFDS interaction is difficult to predict. For these different reasons, expectations based on the wealth of knowledge accumulated for NFDS among alleles within sexual species and among emerging asexual lineages is unlikely to be sufficient to draw global, interspecific conclusions about the role of NFDS for long-term coexistence.

To address this question, we study the long-term coexistence between two bacteria species, *Escherichia coli* (hereafter *E. coli* or *E*) and *Citrobacter freundii* (hereafter *C. freundii* or *C*) grown on a medium with two carbon sources, glucose and citrate. *E* is particularly efficient at using glucose, but cannot take up citrate under aerobic conditions, while *C* can use both carbon sources. As we show, *E* and *C* can coexist by NFDS. We investigate the evolution of their NFDS patterns in multiple replicates in a ca. 900 generations experimental evolution setting. In particular, we investigate whether different abiotic conditions (different concentration of an antibiotic, nalidixic acid) change long-term coexistence, as would be expected if different environments represent different adaptive challenges to the two coevolving species.

Material and methods

Strains and experimental evolution

In our experiment, NFDS occurs between one Lenski's long term experiment derived *E. coli* strain (Lenski and Travisano 1994) (*E*) constitutively expressing yellow fluorescent proteins (YFP) that has been previously evolved in the presence of nalidixic acid (Nal) (Gallet et al. 2012; Harmand et al. 2017, 2018) and one *C. freundii* strain (*C*) at very low starting frequency resulting from contamination of *E* glycerol stocks. Hence, *E* is well adapted to the experimental conditions in the absence of *C* whereas these conditions are new for *C*. Bacterial populations were propagated through daily 100-fold dilutions (Sup. Methods) into fresh Davis minimal medium containing 250 µg/mL of glucose and Nal at six different concentrations: 0, 3, 8, 20, 100 and 200 µg/mL (referred below to as Nal0, Nal3, etc.). We followed the frequency of the coevolving species in 44 coevolutionary replicates (hereafter CRep, 8 per dose of Nal, and 4 in absence of Nal). The frequencies of *E* and *C* were estimated for each CRep at ca. 0, 200, 550 and 870 generations using flow cytometry. See supplementary methods for details about the coevolution protocol and frequency measures. *E* and *C* were isolated based on phenotypic differences between the two species. Their growth patterns on glucose, on different doses of citrate or on filtrate of medium

where the other species had grown were measured following optical density using standard methods (Sup. Methods).

NFDS patterns and fitness measures

Two CRep from Nal20 (CRep20A and CRep20B) were selected to investigate detailed variations in the NFDS patterns during coevolution. Six independent clones of both *C* and *E* type were isolated from those CRep at time 0, 214 and 870 generations and mixed to constitute *E* and *C* lines representative of each time point. Variations of the NFDS patterns were investigated by performing five different series of competitions: 1) *E* against *C* at time zero (*E0* against *C0*), 2) *E* against *C* at 214 generations (*E2* against *C2*), 3) *E* against *C* at 870 generations (*E8* against *C8*), 4) *E0* against *C8*, and 5) *E8* against *C0*. The first three series should indicate whether the interaction changed during coevolution, while the last two should indicate how each species contributed to that change. Separate overnight cultures of the *E* and *C* lines were mixed with a large range of initial frequencies and mixes were incubated for 24h in the same conditions as the experimental evolution. Selection coefficients per generation were calculated in a standard way, as in Harmand *et al.* (2018), eq. (1), using frequency variation over 24h (supp. methods).

Results

NFDS patterns evolved rapidly and consistently across abiotic conditions

The two species were still coexisting in 39 CRep out of 44 at generations 200, 550 and 870 (Fig. 2). The frequency of *E* decreased very consistently across replicates. This decrease was also consistently (much) stronger for increasing Nal concentrations (Fig. 2). A clear NFDS pattern was present at generations 0 and 870 for CRep20A and CRep20B (Fig. 3). Remarkably, these NFDS patterns were highly nonlinear, with a steep fitness change near frequency = 0 or 1. In the five remaining CRep (one at Nal0, two at Nal3, one at Nal100 and one at Nal200), *C* was never detected, and probably did not establish from the start (supp. methods).

Fig. 3 shows that the NFDS patterns changed dramatically along coevolution in CRep20A and CRep20B replicates investigated in detail. Their shape was not strongly changed between initial and final time, but was shifted significantly downwards (which is analogous to a change in intercept as illustrated in Fig. 1). Consistent with this shift, *E* frequency declined in these replicates. In other replicates, where we did not investigate the NFDS pattern, *E* frequency also declined regularly. This decline is consistently more pronounced at increasing Nal concentrations

(Fig. 2). CRep20A and CRep20B do not particularly stand out: they are just two replicates among many others showing a very similar trend in frequency variation.

Evolution of NFDS pattern is mostly driven by the adaptation of *C. freundii*

We performed competitions at generations 0, 214 and 870 as well as time-shifted competitions in order to assign specific patterns of variation in NFDS patterns to *E* or *C* evolution. Competitions between *E0* and *C8* should indicate whether the evolution of *C* was responsible for the change in NFDS pattern, and the reciprocal competition should measure how much change of the pattern was due to the evolution of *E*. Fig. 3 shows that *E8-C0* pattern is nearly identical to the *E0-C0* pattern, and that *E0-C8* patterns are nearly identical to the *E8-C8* pattern. This indicates that *E* did not evolve much and therefore that nearly all the evolutionary changes modifying the NFDS pattern occurred in *C*. The growth curves of isolated *C* and *E* lines confirm that *C* was adapting rapidly during coevolution. In particular, these growth curves show a reduction in *C* lag time for citrate consumption (CRep20A and B, Fig. 4) and improved growth on glucose (CRep20B, Fig. 4). In contrast, *E* showed no obvious adaptation to the abiotic conditions. Hence, the variation of the NFDS is almost entirely due to the evolution of *C*.

The shapes of the NFDS patterns at initial and final time are very similar (Fig. 3). The main difference is an overall shift downwards, as would be expected if *C* accumulated many more unconditionally beneficial mutations over this period. Here we refer as unconditionally beneficial to mutations that confer the same fitness advantage at all frequencies. However, this interpretation is not correct. At intermediate time, the NFDS patterns show a very different shape (see NFDS patterns at generation 214 in Fig. 5). They are only shifted downwards for large starting frequencies of *E*, not for small frequencies. The modification of the NFDS pattern therefore occurred in a stepwise fashion. *C* first acquired mutations that presented an advantage when *C* was rare. In a second step, other beneficial mutations occurred that were beneficial in a higher range of *C* frequencies. The same pattern holds very consistently for CRep20A and CRep20B.

Ecological context of the frequency-dependent selection

C presents a diauxic growth (i.e. a growth curve with two exponential phases on two different resources), but *E* does not (Fig 4). *C* overall carrying capacity increases linearly with citrate concentration, confirming that *C* consumes citrate. Citrate concentration has almost no effect on the first growth phase of *C*, indicating that *C* consumes glucose first (Fig S2). *E* maximal carrying capacity occurs at 100% citrate (i.e. the concentration corresponding to that of the experimental evolution medium). At other citrate concentrations, this carrying capacity is smaller, but the difference is modest in all cases. This small variation does indicate that citrate plays a role in *E*

metabolism, but not as a resource (e.g. pH buffering). The modest effect of citrate concentration on *E* carrying capacity did not change between generation 0 and 870 (all these results are shown in Fig S2). At the start of the coevolution, *C* growth achieved on glucose is always lower than *E* growth, indicating that *C* has a lower efficiency on glucose. To achieve a larger overall carrying capacity than *E*, *C* requires some citrate (at least ~one quarter of the concentration in the DM250, Fig S1a). At generation 870, these comparisons cannot be made easily as the diauxic shift for *C* cannot be well identified (see for instance Fig 4). In most *C* lines, the lag time of switching from glucose to citrate resource becomes hardly detectable. Finally, *E* did not grow in the filtrated medium produced after a growth cycle of *C* (while *C* could use citrate in the reverse situation, Suppl. results.). This indicates that they do not excrete byproducts that are left undigested. This observation does not rule out the possibility that some metabolites are excreted and then reabsorbed and consumed later (e.g. acetate can be produced and temporarily excreted).

Modelling non-linear NFDS patterns

We investigated theoretically the NFDS patterns that can be obtained in competition scenarios of two strains with two resources and diauxy. We detail this model in Appendix 1 and Fig S1 presents it graphically. Figure 6a-c illustrates the NFDS patterns expected under one-niche, two-niches and three-niches models. In the one niche model, the NFDS patterns emerge from a differential specialization on growth rate and conversion efficiency for two types exploiting the same resource. The two niches model corresponds to the Levene's model (1953) with two types competing on two resources. Finally, in the three niches model, there are two resources/niches, but a third one is created by an anticipated metabolic switch of one type to the second resource before the first resource is depleted (i.e. the lag phase on the second resource starts earlier by a quantity Δt). The other type then has a 'private' third niche corresponding to the leftover of the first resource.

Interestingly, the NFDS patterns of this third model are generally consistent with the overall "S-shape" of the NFDS patterns observed with strong curvature at extreme frequencies (Fig. 3). The model can further indicate ways to mimic the observed NFDS pattern evolution through time (Fig 6d). Initially, increasing *C* citrate conversion efficiency can shift down the NFDS pattern at high frequency of *E* (as observed at generation 214 for CRep20A and CRep20B). Then, *C* may evolve to consume more glucose, switching to citrate closer to the time of glucose depletion (smaller Δt). This change favors *C* when frequent while maintaining a small 'private niche' for *E*, and an upward NFDS curvature at very low frequencies of *E* (as observed at generation 870 for CRep20A and CRep20B), hence preserving *E* and *C* coexistence. The model also shows that *C* growth rate and lag time on citrate do not change selection coefficients against *E,* once all resources are exhausted.

Indeed these parameters only influence how fast citrate is consumed, which is irrelevant to *E* that does not consume citrate.

Discussion

Interactions between co-evolving species evolve quickly, but can be maintained through nonlinear NFDS patterns

In this study, we investigated the long-term NFDS coexistence of two species. Following the scenario developed in the introduction, we hypothesized that the two species may not coexist in the long-term, especially if they present asymmetrical rates of adaptation (Fig 1c), as expected for divergent species. Consistent with this scenario, one species (*C. freundii*) evolved at a considerably faster rate than the other (*E.coli*), and became dominant in most of the coevolving cultures with antibiotics (Fig. 2). The shift in the NFDS pattern is rapid so that the frequency of the two species do not even have time to equilibrate at the frequency where their fitness is equal: by the time this frequency is reached, the NFDS has further shifted down so that *E* is always more frequent than would be expected by the current NFDS pattern. This is observed for both CRep20A and CRep20B at intermediate and final times (Fig. 3, 5). The rate of change of NFDS patterns is here somewhat faster (at the scale of 100s of generations) than those observed in the case of emerging polymorphism within an asexual species (see e.g. the changes occurring at ~500 generation scale in Rozen and Lenski 2000). However, in those cases where a polymorphism emerges within asexual species, such an asymmetry quickly favoring one genotype is unexpected since the coevolving genotypes are initially identical, save for a handful of mutations unlikely to drastically favor one at the expense of the other. In our case, *E* and *C* are genetically largely divergent, and did not have the same history of adaptation. *E* was initially relatively well adapted to the environment, due to 10,000 generations of evolution in similar conditions in DM25, and then ~500 generations in DM250-Nal (Harmand et al. 2018). Because adaptation most often shows a pattern of diminishing returns (Lenski and Travisano 1994; Elena and Lenski 2003), *E* was most probably not prone to important and rapid further adaptation to the abiotic conditions (including to the Nal antibiotic, Harmand et al. 2018). In contrast, *C* had probably not been previously exposed to serial batch culture in minimal medium (although the history of this strain cannot be established), and hence was prone to faster and larger adaptive changes in those new conditions. Such asymmetry in adaptive responses are likely to be pervasive among interacting species in many natural situations, for example among populations that were temporarily isolated or brought into contact secondarily or during invasion events. In those cases, long-term species co-existence can be maintained through NFDS interactions only if those interactions are resilient to

further adaptation of these species, meaning that observation of NFDS interactions at one given evolutionary time does not guarantee long-term coexistence. In our case, and despite a strong asymmetry in rates of adaptation of the two interacting species, they were still coexisting after 870 generations (in the 39 replicates where *C* initially established). This striking outcome was due to the particular S-shape of the NFDS patterns with extensive curvature near the fixation points (Fig. 3) protecting *E* from extinction by strongly favoring it when rare. Such "S-shaped" NFDS pattern can considerably extend long-term coexistence of interacting species, as an internal equilibrium can still be preserved even with large shifts in intercepts. This is an important departure from the simplified scenario usually envisioned and illustrated in Fig. 1, where linear NFDS patterns do not strongly protect competing types against extinction if one is evolving quicker. Hence, the shape of initial NFDS patterns between interacting types can be qualitatively different among divergent species than among emerging polymorphisms, with a strong consequence on their long-term coexistence.

The evolution of NFDS patterns through time

Asymmetric rates of adaptation to the abiotic conditions between *E* and *C* are clearly not a sufficient explanation for all the results. For CRep20A and B, the NFDS patterns were mainly shifted downwards between the initial and final time points. This pattern would be expected if unconditionally beneficial mutations accumulated in *C*. However, NFDS patterns at an intermediate time (generation 214, Fig 5) showed that, in both cases, the shape of the NFDS changed sequentially, first shifted downward for the range of frequencies where *C* is rare (i.e. on the right of *x*-axis in Fig 5), and then, later, shifted downward for the range of frequencies where *C* is frequent (i.e. on the left of *x*-axis in Fig. 5). This degree of malleability of NFDS patterns is surprising, but not unexpected. Initially, *C* is rare. It will therefore mostly fix mutations that confer an advantage at this frequency (irrespective of their effect when *C* is frequent). Then the equilibrium frequency of *C*, dictated by the NFDS pattern, increases, which triggers the fixation of other mutations that confer an advantage at higher *C* frequency, as is observed. Consequently, the final NFDS pattern appears as shifted down at all frequencies, giving the impression that it was modified by the accumulation of beneficial but frequency–independent mutations. On the contrary, the evolution of the NFDS pattern appears to be highly dynamic. It indicates that many mutations are available but that some confer different selective advantages at different frequencies, providing ample flexibility in the possible evolutionary deformation in the NFDS pattern. Because these mutations influence the shape of the NFDS pattern, and have a frequency-dependent effect, they probably modify the interaction between the two species, rather than being unconditionally beneficial to the laboratory condition. This is a second important departure from the simplified scenario usually envisioned (presented in the introduction and in Fig. 1). Many

mutations with a frequency-dependent effect seem to be available for adaptation, which allows for considerable malleability in the evolution of the shape of NFDS pattern through time, beyond mere changes in intercepts or slopes.

The origin of non-linear NFDS patterns

Different biological mechanisms can lead to NFDS (Table S1), and they can be difficult to tease apart as they can lead to identical NFDS patterns. In our case study, many possibilities can be ruled out (e.g. effect of parasites or predators) and some possibilities are worth discussing. First, NFDS can emerge from environmental heterogeneity (mainly represented here by different resources) provided that relevant fitness trade-offs exist among the different niches, as in Levene's model (Levene 1953; Ravigné et al. 2004). This is a good candidate mechanism in this study since the medium includes two carbon sources, glucose and citrate, on which E and C are known to be specialized, respectively. In particular, E does not usually consume citrate under aerobic conditions (Dimroth 2013), but C does. Second, additional niches can be created by the strains themselves, as e.g. with cross-feeding interactions (Rosenzweig et al. 1994; Treves et al. 1998; Doebeli 2002; Plucain et al. 2014) or detoxification of the environment (Dugatkin et al. 2005; Kelsic et al. 2015). Third, the coexistence can rely on different strategies of exploitation of the same resource via a trade-off between the uptake efficiency and the energetic conversion of a resource. Finally, these mechanisms can be combined. For example, a strain which consumes the resource rapidly but with low efficiency (third mechanism) may be prone to excrete byproducts, which provides an opportunity for cross-feeding interactions (second mechanism).

The NFDS patterns alone do not provide sufficient information to decipher among these mechanisms. Nevertheless, by modelling competition between one diauxic and one non-diauxic species (Fig. S1), we pinpoint likely hypotheses at the basis of the establishment and evolution of the interaction between the two species. First, we showed that an overall "S-shape" of the NFDS patterns can be obtained in a two-resource model only if the diauxic species switches to the second resource before the first one is entirely depleted. The remaining glucose constitutes a private niche to the non-diauxic species that becomes strongly favored when rare. Such a private niche cannot be revealed by growth curves of E and C in isolation (Fig 4). These curves showed that C initially exhibits a clear diauxic growth on two resources and that only C evolved, notably by decreasing the lag on citrate (λ_{C2} smaller). This may erroneously suggest that the evolution of the NFDS pattern mainly rely on this smaller λ_{C2}. However, as shown by our model, such change is neutral with respect to competition with E. It probably only evolved due to within-C competition for citrate consumption. Within-C competition may also be key for the evolution of C anticipated switch since it may be worthwhile for a diauxic species to anticipate the switch to a very abundant

second resource before the first one is entirely depleted. Ultimately, the model showed that it is the time at which *C* initiates its switch to citrate rather than the time it takes to switch that is central for the evolution of NFDS pattern between *E* and *C*. Our modelling clarifies these points. Yet, it is likely that NFDS interactions can be generally more complex than the baseline situation depicted in the model. For instance, in our case study, it is very possible that other intermediate carbon sources (e.g. acetate, succinate) are temporarily excreted and exploited by *E* and *C*. The model also provides keys to pointing the most promising candidate mechanisms that can yield frequency-dependent changes that cannot be summarized by mere changes in intercept as presented in Fig. 1. In our case, such mechanism creates a situation where adaptation in one species indirectly opens a niche for another, in absence of cross-feeding. Further experiments are however required to identify the exact mechanism at work, notably by investigating the competition of the two species on glucose alone, provided that pH buffering in absence of citrate can be controlled for.

NFDS evolution across environments

The evolution of *E* frequency in our experiment was strongly influenced by abiotic environmental conditions (here the concentration of Nal). The patterns of variation are highly regular with respect to the gradient of Nal concentration. The importance of environmental conditions in the emergence or maintenance of biotic interactions has already been pointed out in other experiments (e.g. in Hansen and Hubbell 1980; Healey et al. 2016). These observations suggest that the environmental context can have a large influence on the long-term maintenance of NFDS interactions. This would be easily interpretable if such environmental variation was related to the mechanism of coexistence, for instance the proportion of the different available resources (glucose or citrate). But this is not the case here: the environmental variable playing such a strong role is the concentration of the antibiotic, which seems entirely unrelated to the mechanism of coexistence and orthogonal to the issue of resource utilization. A possible explanation might be that Nal represents an asymmetrical challenge for *C* and *E*. For instance, contrary to *E*, *C* may be mostly unaffected by the presence of Nal at any concentration (e.g. because of reduced uptake or a Nal-proof gyrase target). Some tests (not shown) indicated that *C* growth rate was not affected, but *E* growth rate reduced with increasing Nal concentration up to 200 μg/mL. Another possibility might be that, fortuitously, Nal resistance in *E* favored *C*. In particular, some (loss-of-function) mutations on enzymes of the Krebs cycle, have been shown to be selected in *E* to resist Nal. Presumably, metabolites that accumulate upstream of the blocks caused by the mutations increase the expression levels of generalist efflux pumps, thereby removing Nal from the organism (Helling and Kukora 1971; Lakshmi and Helling 1976; Helling et al. 2002). This resistance mechanism, however, reduces metabolic efficiency and leads to the excretion of intermediate

metabolite that could be exploited by *C*. In all cases, adding a direct advantage to *C* with increasing Nal concentration is sufficient to explain why *E* equilibrium frequency is lower at increasing Nal doses (scenario modelled and shown in Fig. 6e). Irrespective of the exact underlying mechanism, our results show that environmental conditions that are *a priori* unrelated to the mechanism of coexistence can largely impact the evolution of NFDS patterns.

The maintenance of rare species

The persistence of rare species in communities is often difficult to understand, as they should be very vulnerable to stochastic perturbations or to slight adaptation of their competitor. The occurrence of a sharply increasing selective advantage at very low frequencies, as demonstrated in our case, could explain these observations. This increased coexistence timespan may provide sufficient time for further niche specialization, and eventually stabilization of interactions among coevolving competitors. Here we showed that this non-linearity may occur because of incomplete exploitation of resources by the more generalist species. There is indeed a strong selection pressure within that generalist population (here *C* that consumes both glucose and citrate) to switch resources when the first resource starts to be too rare to be worth exploiting. This inevitably opens a private niche for a more specialized species that can persist in the long term at very low frequency. This process of indirect niche construction may provide a general mechanism to explain persistence of rare species in ecological systems.

Acknowledgments

We thank M.-P. Dubois and R. Zahab for lab management and the Montpellier Ressources Imagerie (MRI) platform. We thank R. Zahab for technical support and help with the experiments. We also wish to thank E. Lievens and three anonymous reviewers for very helpful suggestions on the manuscript and R. Gallet, G. Martin, S. Bedhomme, P. Labbé, and N. Bierne for discussions. The original strain RELB 4536 was kindly provided by Richard Lenski's lab. This work was supported by a PhD grant from French ministry of research to NH, and the ANR SilentAdapt to T.L.

References

Allen, J. A. 1988. Frequency-dependent selection by predators. Philos. Trans. R. Soc. Lond. B. Biol. Sci. 319:485–503.

Ayala, F. J., and C. A. Campbell. 1974. Frequency-dependent selection. Annu. Rev. Ecol. Syst. 115–138.

Barnard, C. J., and R. M. Sibly. 1981. Producers and scroungers: A general model and its application to captive flocks of house sparrows. Anim. Behav. 29:543–550.

Bell, G. 2008. Selection: the mechanism of evolution, second edition. Oxford University Press.

Billiard, S., M. Lopez-Villavicencio, B. Devier, M. Hood, C. Fairhead, and T. Giraud. 2011. Having sex, yes, but with whom? Inferences from fungi on the evolution of anisogamy and mating types. Biol. Rev. 86:421–442.

Blount, Z. D., J. E. Barrick, C. J. Davidson, and R. E. Lenski. 2012. Genomic analysis of a key innovation in an experimental Escherichia coli population. Nature 489:513–8.

Blount, Z. D., C. Z. Borland, and R. E. Lenski. 2008. Historical contingency and the evolution of a key innovation in an experimental population of *Escherichia coli*. Proc. Natl. Acad. Sci. U. S. A. 105:7899–906.

Bonsall, M. B. 2006. Longevity and ageing: appraising the evolutionary consequences of growing old. Philos. Trans. R. Soc. Lond. B. Biol. Sci. 361:119–135.

Borghans, J. A. M., J. B. Beltman, and R. J. De Boer. 2004. MHC polymorphism under host-pathogen coevolution. Immunogenetics 55:732–739.

Bürger, R. 2010. Evolution and polymorphism in the multilocus Levene model with no or weak epistasis. Theor. Popul. Biol. 78:123–138.

Castric, V., and X. Vekemans. 2004. Plant self-incompatibility in natural populations: a critical assessment of recent theoretical and empirical advances. Mol. Ecol. 13:2873–2889.

Clarke, B. 1962. Balanced polymorphism and the diversity of sympatric species. Pp. 47–70 *in* D. Nichols, ed. Taxonomy and Geography. Systematics Association, Oxford.

Cordero, O. X., and M. F. Polz. 2014. Explaining microbial genomic diversity in light of evolutionary ecology. Nat Rev Microbiol 12:263–273.

Débarre, F., and T. Lenormand. 2011. Distance-limited dispersal promotes coexistence at habitat boundaries: reconsidering the competitive exclusion principle. Ecol. Lett. 14:260–6.

Devier, B., G. Aguileta, M. E. Hood, and T. Giraud. 2009. Ancient trans-specific polymorphism at pheromone receptor genes in basidiomycetes. Genetics 181:209–223.

Dimroth, P. 2013. Molecular basis for bacterial growth on citrate or malonate. EcoSalPlus 1–36.

Doebeli, M. 2002. A model for the evolutionary dynamics of cross-feeding polymorphisms in microorganisms. Popul Ecol 44:59–70.

Dugatkin, L. A., M. Perlin, J. S. Lucas, and R. Atlas. 2005. Group-beneficial traits, frequency-dependent selection and genotypic diversity: an antibiotic resistance paradigm. Proc. Biol. Sci. 272:79–83.

Elena, S. F., and R. E. Lenski. 2003. Evolution experiments with microorganisms: the dynamics and genetic bases of adaptation. Nat. Rev. Genet. 4:457–69.

Felsenstein, J. 2017. Theoretical evolutionary genetics. J. Felsenstein, University of Washington, Seatle.

Fincke, O. M. 2004. Polymorphic signals of harassed female odonates and the males that learn

them support a novel frequency-dependent model. Anim. Behav. 67:833–845.

Friesen, M. L., G. Saxer, M. Travisano, and M. Doebeli. 2004. Experimental evidence for sympatric ecological diversification due to frequency-dependent competition in *Escherichia coli*. Evolution 58:245.

Gallet, R., T. F. Cooper, S. F. Elena, and T. Lenormand. 2012. Measuring selection coefficients below 10^{-3}: Method, Questions, and Prospects. Genetics 190.

Gigord, L. D., M. R. Macnair, and A. Smithson. 2001. Negative frequency-dependent selection maintains a dramatic flower color polymorphism in the rewardless orchid *Dactylorhiza sambucina* (L.) Soo. Proc. Natl. Acad. Sci. U. S. A. 98:6253–6255.

Goldford, J. E., N. Lu, D. Bajić, S. Estrela, M. Tikhonov, A. Sanchez-Gorostiaga, D. Segrè, P. Mehta, and A. Sanchez. 2018. Emergent simplicity in microbial community assembly. Science 361:469–474.

Good, B. H., M. J. McDonald, J. E. Barrick, R. E. Lenski, and M. M. Desai. 2017. The dynamics of molecular evolution over 60,000 generations. Nature 551:45–50.

Gross, M. R. 1996. Alternative reproductive strategies and tactics: diversity within sexes. Trends Ecol. Evol. 11:92–98.

Haldane, J. B. S., and S. D. Jayakar. 1963. Polymorphism due to selection of varying direction. J. Genet. 58:237–242.

Hansen, S. R., and S. P. Hubbell. 1980. Single-nutrient microbial competition: qualitative agreement between experimental and theoretically forecast outcomes. Science 207:1491–1493.

Harmand, N., R. Gallet, R. Jabbour-Zahab, G. Martin, and T. Lenormand. 2017. Fisher's geometrical model and the mutational patterns of antibiotic resistance across dose gradients. Evolution 71:23–37.

Harmand, N., R. Gallet, G. Martin, and T. Lenormand. 2018. Evolution of bacteria specialization along an antibiotic dose gradient. Evol. Lett. 2:221–232.

Healey, D., K. Axelrod, and J. Gore. 2016. Negative frequency-dependent interactions can underlie phenotypic heterogeneity in a clonal microbial population. Mol. Syst. Biol. 12:877.

Hedrick, P. W. 1978. Genetic variation in a heterogeneous environment. V. Spatial heterogeneity in finite populations. Genetics 89:389–401.

Heino, M., J. A. J. Metz, and V. Kaitala. 1997. Evolution of mixed maturation strategies in semelparous life histories: the crucial role of dimensionality of feedback environment. Philos. Trans. R. Soc. B Biol. Sci. 352:1647–1655.

Helling, R. B., B. K. Janes, H. Kimball, T. Tran, M. Bundesmann, P. Check, D. Phelan, and C. Miller. 2002. Toxic waste disposal in Escherichia coli. J. Bacteriol. 184:3699–703.

Helling, R. B., and J. S. Kukora. 1971. Nalidixic acid-resistant mutants of *Escherichia coli* deficient in isocitrate dehydrogenase. J. Bacteriol. 105:1224–1226.

Helling, R., C. Vargas, and J. Adams. 1987. Evolution of *Escherichia coli* during growth in a constant environment. Genetics 116:349–358.

Joron, M., and J. L. B. Mallet. 1998. Diversity in mimicry: Paradox or paradigm? Trends Ecol. Evol. 13:461–466.

Karasov, T. L., J. M. Kniskerb, L. Gao, B. DeYoung, J. Ding, U. Dubiella, R. O. Lastra, S. Nallu, F. Roux, R. W. Innes, L. G. Barrett, R. R. Hudson, and J. Bergelson. 2014. The long-term maintenance of a resistance polymorphism through diffuse interactions. Nature 512:436–440.

Kelsic, E. D., J. Zhao, K. Vetsigian, and R. Kishony. 2015. Counteraction of antibiotic production and

493 degradation stabilizes microbial communities. Nature 521:516–519.

494 Lakshmi, T. M., and R. B. Helling. 1976. Selection for citrate synthase deficiency in icd mutants of
495 *Escherichia coli*. J. Bacteriol. 127:76–83.

496 Le Gac, M., J. Plucain, T. Hindre, R. E. Lenski, and D. Schneider. 2012. Ecological and evolutionary
497 dynamics of coexisting lineages during a long-term experiment with *Escherichia coli*. Proc.
498 Natl. Acad. Sci. 109:9487–9492.

499 Lenormand, T. 2012. From local adaptation to speciation: specialization and reinforcement. Int. J.
500 Ecol. 2012:e508458.

501 Lenski, R. E., and M. Travisano. 1994. Dynamics of adaptation and diversification: a 10,000-
502 generation experiment with bacterial populations. Proc Natl Acad Sci U S A 91:6808–6814.

503 Levene, H. 1953. Genetic equilibrium when more than one ecological niche is available. Am. Nat.
504 87:331–333.

505 Levin, B. 1972. Coexistence of Two Asexual Strains on a Single Resource. Science 175:1272–1274.

506 Levin, B. R. 1988. Frequency-dependent selection in bacterial populations. Philos. Trans. R. Soc.
507 Lond. B. Biol. Sci. 319:459–472.

508 Lewontin, R. C. 1958. A General Method for Investigating the Equilibrium of Gene Frequency in a
509 Population. Genetics 43:419–34.

510 Maddamsetti, R., R. E. Lenski, and J. E. Barrick. 2015. Adaptation, clonal interference, and
511 frequency-dependent interactions in a long-term evolution experiment with *Escherichia coli*.
512 Genetics 200:619–631.

513 Manhart, M., B. V. Adkar, and E. I. Shakhnovich. 2018. Trade-offs between microbial growth phases
514 lead to frequency-dependent and non-transitive selection. Proc. R. Soc. B Biol. Sci.
515 285:20172459.

516 Mazancourt, C. de, and U. Dieckmann. 2004. Trade-Off Geometries and Frequency-Dependent
517 Selection. Am. Nat. 164:765–778.

518 O'Connell, L. M., and M. O. Johnston. 1998. Male and Female Pollination Success in a Deceptive
519 Orchid, a Selection Study. Ecology 79:1246–1260.

520 Oaten, A., and W. W. Murdoch. 1975. Functional response and stability in predator-prey systems.
521 Am. Nat. 109:289–298.

522 Olendorf, R., F. H. Rodd, D. Punzalan, A. E. Houde, C. Hurt, D. N. Reznick, and K. a Hughes. 2006.
523 Frequency-dependent survival in natural guppy populations. Nature 441:633–636.

524 Penn, D. J., and W. K. Potts. 1999. The evolution of mating preferences and major
525 histocompatibility complex genes. Evolution 153:145–164.

526 Plucain, J., T. Hindré, M. Le Gac, O. Tenaillon, S. Cruveiller, C. Médigue, N. Leiby, W. R. Harcombe, C.
527 J. Marx, R. E. Lenski, and D. Schneider. 2014. Epistasis and allele specificity in the emergence
528 of a stable polymorphism in *Escherichia coli*. Science 343:1366–1369.

529 Rainey, P. B., and M. Travisano. 1998. Adaptive radiation in a heterogeneous environment. Nature
530 394:69–72.

531 Ravigné, V., I. Olivieri, and U. Dieckmann. 2004. Implications of habitat choice for protected
532 polymorphisms. Evol. Ecol. Res. 6:125–145.

533 Reusch, T. B. H., M. A. Häberli, P. B. Aeschlimann, and M. Milinski. 2001. Female sticklebacks count
534 alleles in a strategy of sexual selection explaining MHC polymorphism. Nature 414:300–302.

535 Rosenzweig, R. F., R. R. Sharp, D. S. Treves, and J. Adams. 1994. Microbial evolution in a simple
536 unstructured environment: Genetic differentiation in *Escherichia coli*. Genetics 137:903–

917.

Rozen, D. E., and R. E. Lenski. 2000. Long-Term experimental evolution in *Escherichia coli*. VIII. Dynamics of a balanced polymorphism. Am. Nat. 155:24–35.

Rozen, D. E., L. McGee, B. R. Levin, and K. P. Klugman. 2007. Fitness costs of fluoroquinolone resistance in *Streptococcus pneumoniae*. Antimicrob. Agents Chemother. 51:412–416.

Rozen, D. E., N. Philippe, J. Arjan de Visser, R. E. Lenski, and D. Schneider. 2009. Death and cannibalism in a seasonal environment facilitate bacterial coexistence. Ecol. Lett. 12:34–44.

Sinervo, B., and C. M. Lively. 1996. The rock-paper-scissors game and the evolution of alternative male strategies. Nature 380:240–243.

Takahashi, Y., and M. Kawata. 2013. A comprehensive test for negative frequency-dependent selection. Popul. Ecol. 55:499–509.

Takahata, N., and M. Nei. 1990. Allelic genealogy under overdominant and frequency-dependent selection and polymorphism of major histocompatibility complex loci. Genetics 124:967–978.

Těšický, M., and M. Vinkler. 2015. Trans-Species Polymorphism in Immune Genes: General Pattern or MHC-Restricted Phenomenon? J. Immunol. Res. 2015:838035.

Thijs, H., J. R. Shann, and J. D. Weidenhamer. 1994. The effect of phytotoxins on competitive outcome in a model system. Ecology 75:1959–1964.

Treves, D. S., S. Manning, and J. Adams. 1998. Repeated evolution of an acetate-crossfeeding polymorphism in long-term populations of *Escherichia coli*. Mol. Biol. Evol. 15:789–97.

Turner, P. E., V. Souza, and R. E. Lenski. 1996. Tests of ecological mechanisms promoting the stable coexistence of two bacterial genotypes. Ecology 77:2119–2129.

van Diepen, L. T. A., Å. Olson, K. Ihrmark, J. Stenlid, and T. Y. James. 2013. Extensive Trans-Specific Polymorphism at the Mating Type Locus of the Root Decay Fungus Heterobasidion. Mol. Biol. Evol. 30:2286–2301. Oxford University Press.

Wang, J., E. Atolia, B. Hua, Y. Savir, R. Escalante-Chong, and M. Springer. 2015. Natural variation in preparation for nutrient depletion reveals a cost-benefit tradeoff. PLoS Biol. 13:1–31.

Weeks, A. R., and A. a Hoffmann. 2008. Frequency-dependent selection maintains clonal diversity in an asexual organism. Proc. Natl. Acad. Sci. U. S. A. 105:17872–17877.

Figure Legends

Figure 1. Evolution of frequency-dependence and long-term coexistence. The figure illustrates patterns of negative frequency-dependent selection between types (NFDS, left panels) and the corresponding frequency variation in co-existing populations (right panels, the time scale is such that mutations appear as instantaneously fixed). Basically, NFDS can be described as a negative linear dependence between the selection coefficient of one type (*y*-axis) against its frequency (*x*-axis) which defines the equilibrium frequency at which both types can eventually co-exist indefinitely (i.e. where the NFDS line intersects the *x*-axis). However, this selective equilibrium may be displaced by further mutations: Panels (a): In sexual species, a new allele at one polymorphic locus is supposed to have a limited impact on the equilibrium frequency because recombination will disconnect such allele at one locus from other mutations in the genome; Panels (b): In de novo divergent asexual species where recombination is absent, both emerging types share similar mutational opportunity to further adapt to their common environment at a whole genome scale. Any beneficial mutation fixed in one lineage will shift the NFDS line either up or down depending in which type such mutation arise (on fig. 1b, see e.g. beneficial mutations 2 and 3 arising in type A shifting up the NFDS line whereas beneficial mutations 1 and 4 arising in type B shift it down). Overall, 2 types adapting at a similar rate will exhibit successive up and down variations of the NFDS line, temporally changing their equilibrium frequency but not disrupting their long-term coexistence; Panels (c): When NFDS occurs between types from 2 divergent species with an asymmetric rate of adaptation to a common environment, the NFDS line will shift up or down but to an extent causing the selective fixation of the type more prone to adapt to the common environment (on fig. 1c see e.g mutations 1, 3, 4 with large effect in B that are not ultimately counterbalanced by mutation 2 with smaller effect in A). Panel (d): The previous panels only consider the fixation of beneficial mutations uniformly affecting the fitness of one type independently of its frequency. However, mutation contributing to the specialization of one type to a dedicated ecological niche may alternatively affect the slope of the NFDS line instead of the equilibrium frequency (see Fig. 1d). Such a mutation may occur in previous cases (a, b, c) with increased slope improving long-term coexistence since mutation with a larger effect will be required to switch the NFDS line to a point where one type will be selectively outcompeted.

Figure 2. Evolution of the proportion (y-axis in %) of *E. coli* against *C. freundii* throughout the coevolution at different antibiotic concentrations (color code indicated in the figure for the different Nal concentrations). In panel (a), mean values and standard deviations are calculated per antibiotic dose (8 CRep per Nal dose, but 4 in Nal0). Values for each CRep are shown in panel (b). Frequency estimates were obtained using samples of 100,000 cells (*E. coli* frequency was computed as the proportion of YFP fluorescent cells).

Figure 3: Negative frequency-dependent selection patterns between *E. coli* and *C. freundii* at initial (0) (grey dots) and final time (8) (black dots) of the coevolution from two sets of lines co-evolved in DM250-Nal20 (CRep20A and B, top and bottom panels, respectively). Triangles represent the crossed-time competitions. Each point is the selection coefficient of one competition, some of which were done in duplicate (same *E* frequency). Green marks on the *x*-axis represent the frequency of *E* measured in the mixes at initial (higher values) and final time (lower values) of the coevolution.

Figure 4: Growth curves in DM250-Nal20 of *E. coli* and *C. freundii* lines isolated from CRep20A and CRep20B throughout the coevolution (grey gradient). Growth curves were repeated four times, resulting in very similar curves, but for the clarity of the figure we selected one representative set. The optical density (OD) was measured at regular intervals of 10 minutes and each dot corresponds to one measure.

Figure 5: Transient deformation of the NFDS pattern at generation 200 (black squares) compared to generation 0 (light grey dots) for CRep20A and CRep20B replicates. This deformation has almost completely disappeared at generation 870 (not represented here for clarity, see Fig. 3).

Figure 6: NFDS patterns obtained by modeling competition between *E* and *C* types. The *x*-axis represents the frequency of *E* (from 0 to 1), and the *y*-axis the selection coefficient of *E* against its competitor *C*. In (**a**), only one resource is considered and *C* initially has a growth advantage over *E* (black line). The grey gradient represents a gradual increase of the efficiency of *E* in energetic conversion that, if large enough, can result in NFDS with an internal frequency equilibrium. In (**b**) and (**c**), two resources are considered. In the baseline situation (black lines) *E* and *C* are equally able to exploit resource 1 (glucose), but *C* can switch to exploit resource 2 (citrate) after glucose is depleted. In these conditions, *C* is favored at all frequencies. (**b**) If *E* evolves a shorter lag phase (or equivalently higher growth rate) when exploiting resource 1, NFDS can emerge as indicated by the grey lines crossing the *x*-axis (the larger the advantage of *E* on resource 1, the lighter the line). (**c**) If *E* parameters remain constant but *C* evolves an anticipated switch to resource 2 (the earlier the switch, the lighter the curve), a "*S*-shaped"-NFDS pattern emerges because *C* switches to citrate before glucose is depleted, hence opening a 'private' niche for *E* on the remaining glucose. This could equivalently be described as a three resources model (citrate, private glucose, shared glucose). In (**d**) and (**e**), the model is used to identify parameters sustaining the observed variations of NFDS patterns during the evolution of CRep. (**d**) Time dynamics in CRep20A (and similarly CRep20B). At time T0, *E* and *C* coexist through NFDS with the *S*-shaped pattern signature as described above. At time T2, the shift down of NDFS pattern mostly at high *E* frequency (step1 arrow, as in Fig. 5) can be obtained by increasing *C* conversion efficiency on citrate, but with an

earlier *C* switch to citrate (leaving more 'private' glucose to *E*). At time T8, the shift-down of NFDS pattern mostly at low *E* frequency (step2 arrow, as in Fig. 3) can be obtained if *C* keeps its conversion efficiency on citrate but evolves back to a later switch to citrate (i.e. leaving less 'private' glucose to *E* compared to T2). (**e**) Negative impact of Nal on *E* frequency at the equilibrium. The shift-down of frequencies with increasing Nal concentrations (as in Fig. 2) can be obtained if Nal imposes a greater reduction of growth rate on glucose (or greater increase of lag phase) for *E* than for *C*. See sup. mat. for more details.

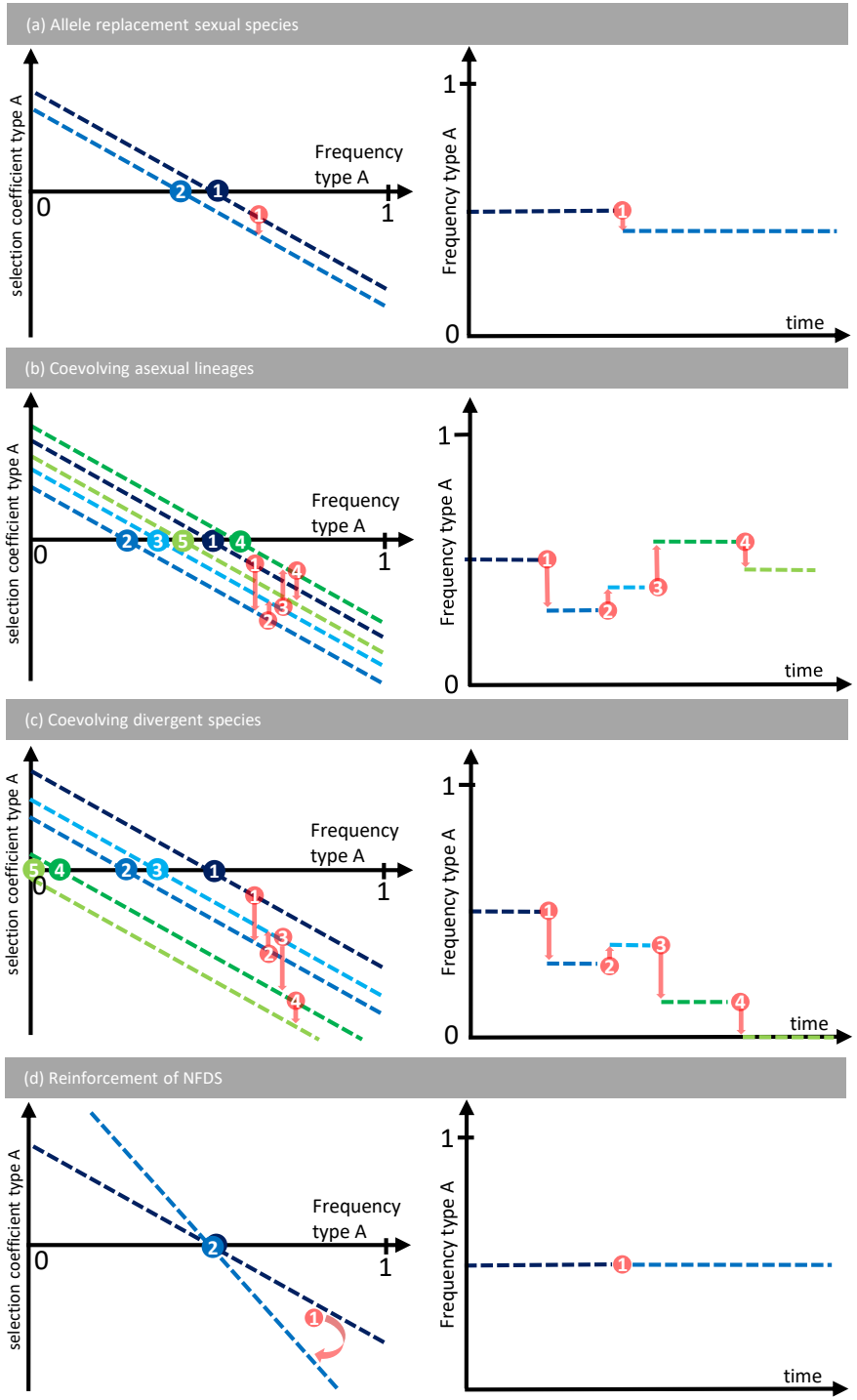
(a) Allele replacement sexual species
selection coefficient type A
Frequency type A
0
1
Frequency type A
1
0
time
(b) Coevolving asexual lineages
selection coefficient type A
Frequency type A
0
1
Frequency type A
1
0
time
(c) Coevolving divergent species
selection coefficient type A
Frequency type A
0
1
Frequency type A
1
0
time
(d) Reinforcement of NFDS
selection coefficient type A
Frequency type A
0
1
Frequency type A
1
0
time

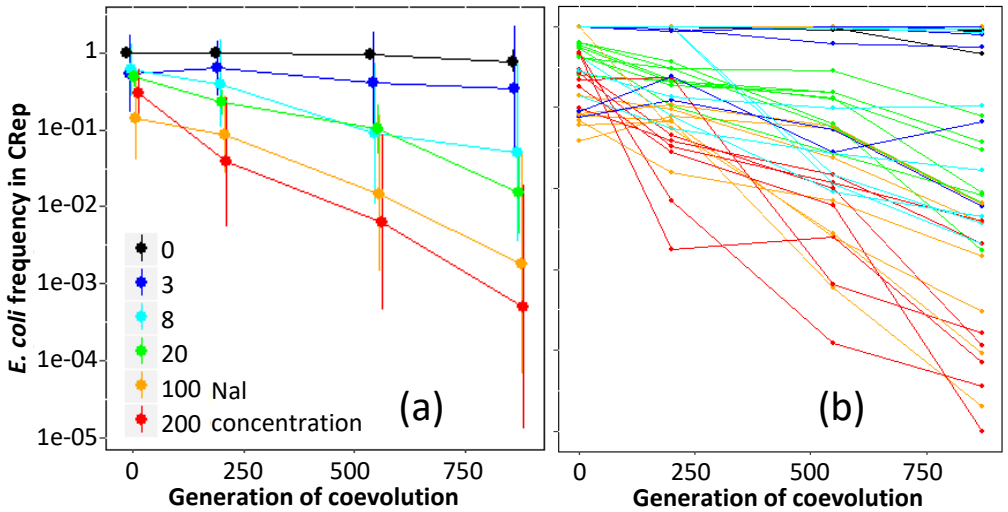
E. coli frequency in CRep
1
1e-01
1e-02
1e-03
1e-04
1e-05
0
3
8
20
100
200
Nal
concentration
(a)
(b)
0
250
500
750
Generation of coevolution
0
250
500
750
Generation of coevolution

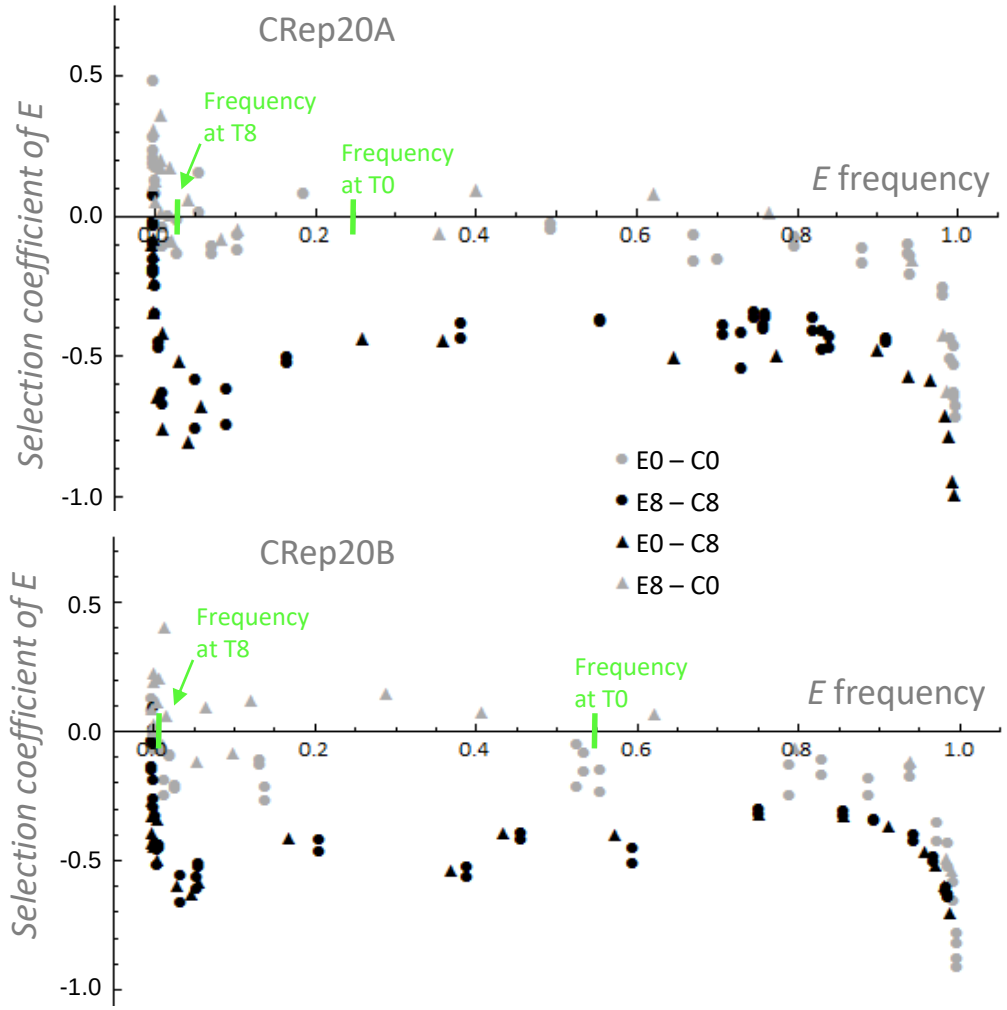
CRep20A
Selection coefficient of E
0.5
0.0
-0.5
-1.0
Frequency at T8
Frequency at T0
E frequency
0.0
0.2
0.4
0.6
0.8
1.0
E0 – C0
E8 – C8
E0 – C8
E8 – C0
CRep20B
Selection coefficient of E
0.5
0.0
-0.5
-1.0
Frequency at T8
Frequency at T0
E frequency
0.0
0.2
0.4
0.6
0.8
1.0

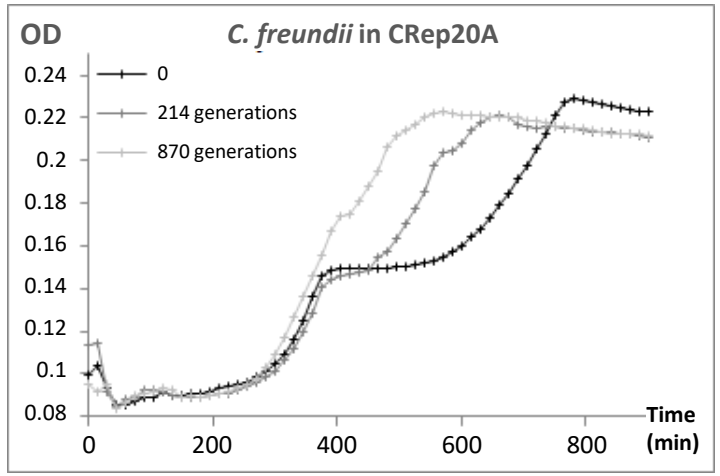
OD
C. freundii in CRep20A
0
214 generations
870 generations
0.24
0.22
0.2
0.18
0.16
0.14
0.12
0.1
0.08
0
200
400
600
800
Time (min)

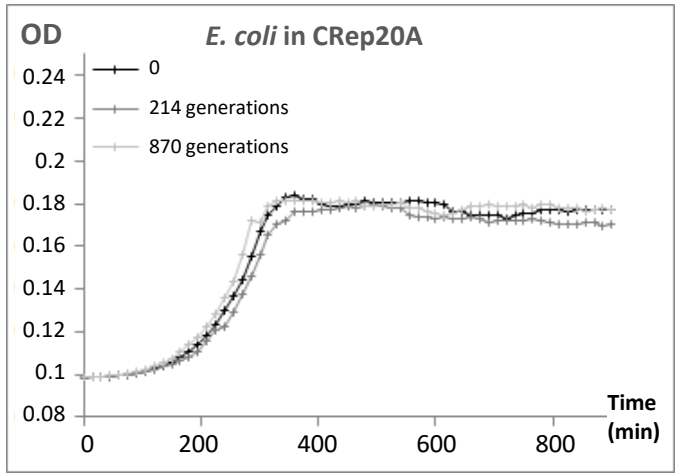
OD
E. coli in CRep20A
0
214 generations
870 generations
0.24
0.22
0.2
0.18
0.16
0.14
0.12
0.1
0.08
0
200
400
600
800
Time (min)

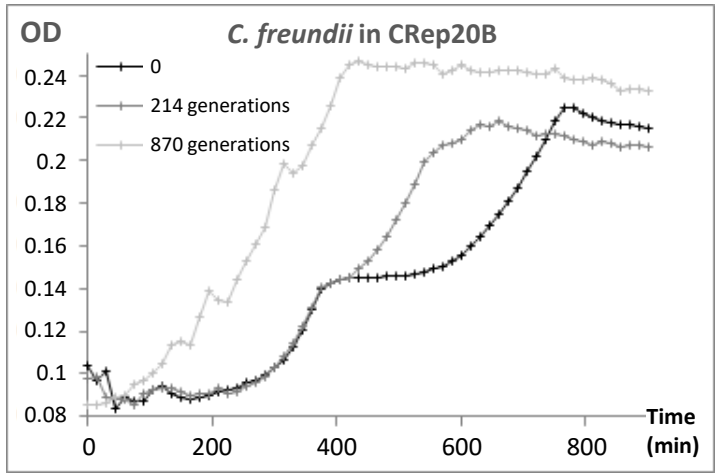
OD
C. freundii in CRep20B
0
214 generations
870 generations
0.24
0.22
0.2
0.18
0.16
0.14
0.12
0.1
0.08
0
200
400
600
800
Time (min)

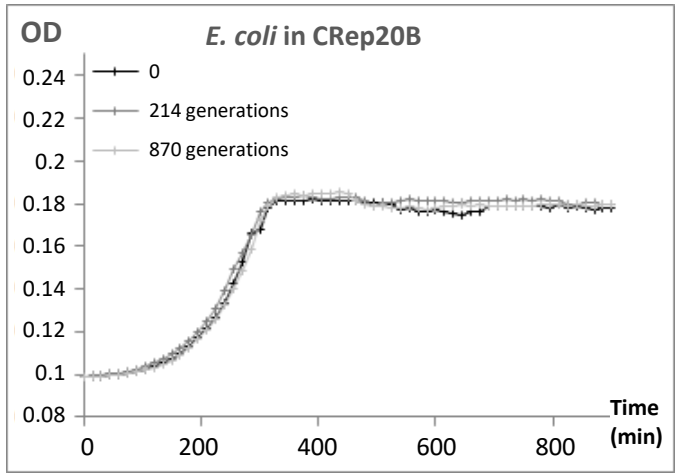
OD
E. coli in CRep20B
0
214 generations
870 generations
0.24
0.22
0.2
0.18
0.16
0.14
0.12
0.1
0.08
0
200
400
600
800
Time (min)

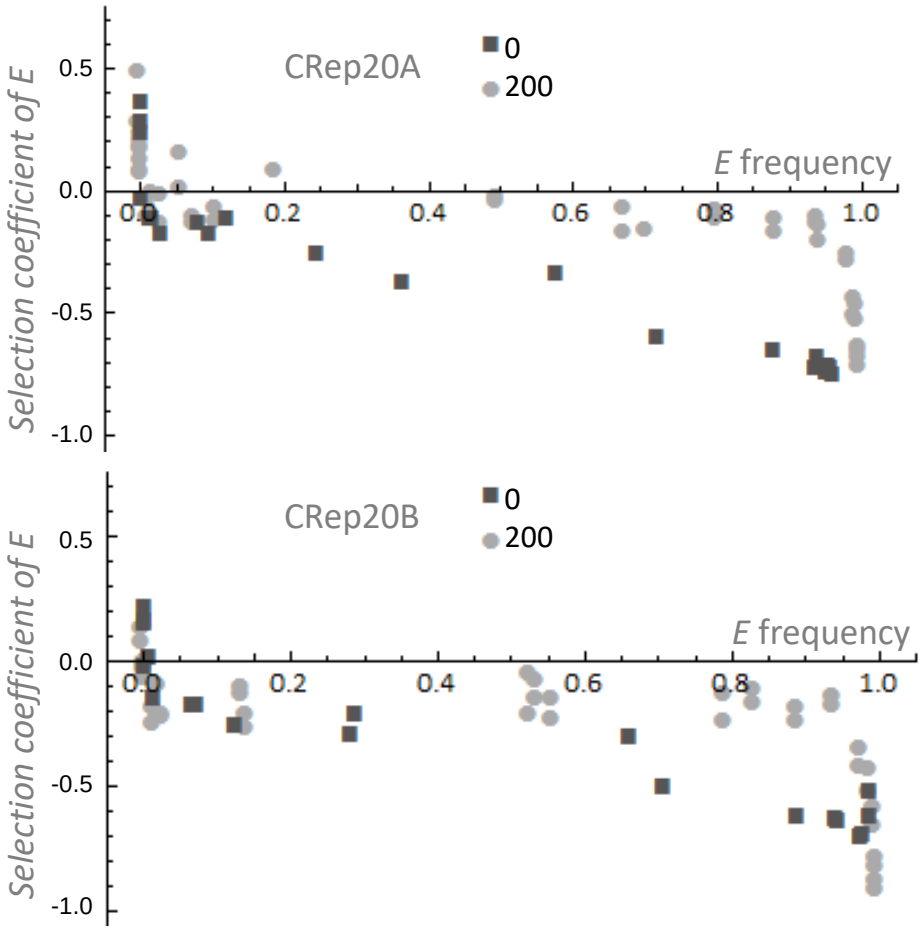
CRep20A
0
200
Selection coefficient of E
E frequency
0.5
0.0
-0.5
-1.0
0.0
0.2
0.4
0.6
0.8
1.0
CRep20B
0
200
Selection coefficient of E
E frequency
0.5
0.0
-0.5
-1.0
0.0
0.2
0.4
0.6
0.8
1.0

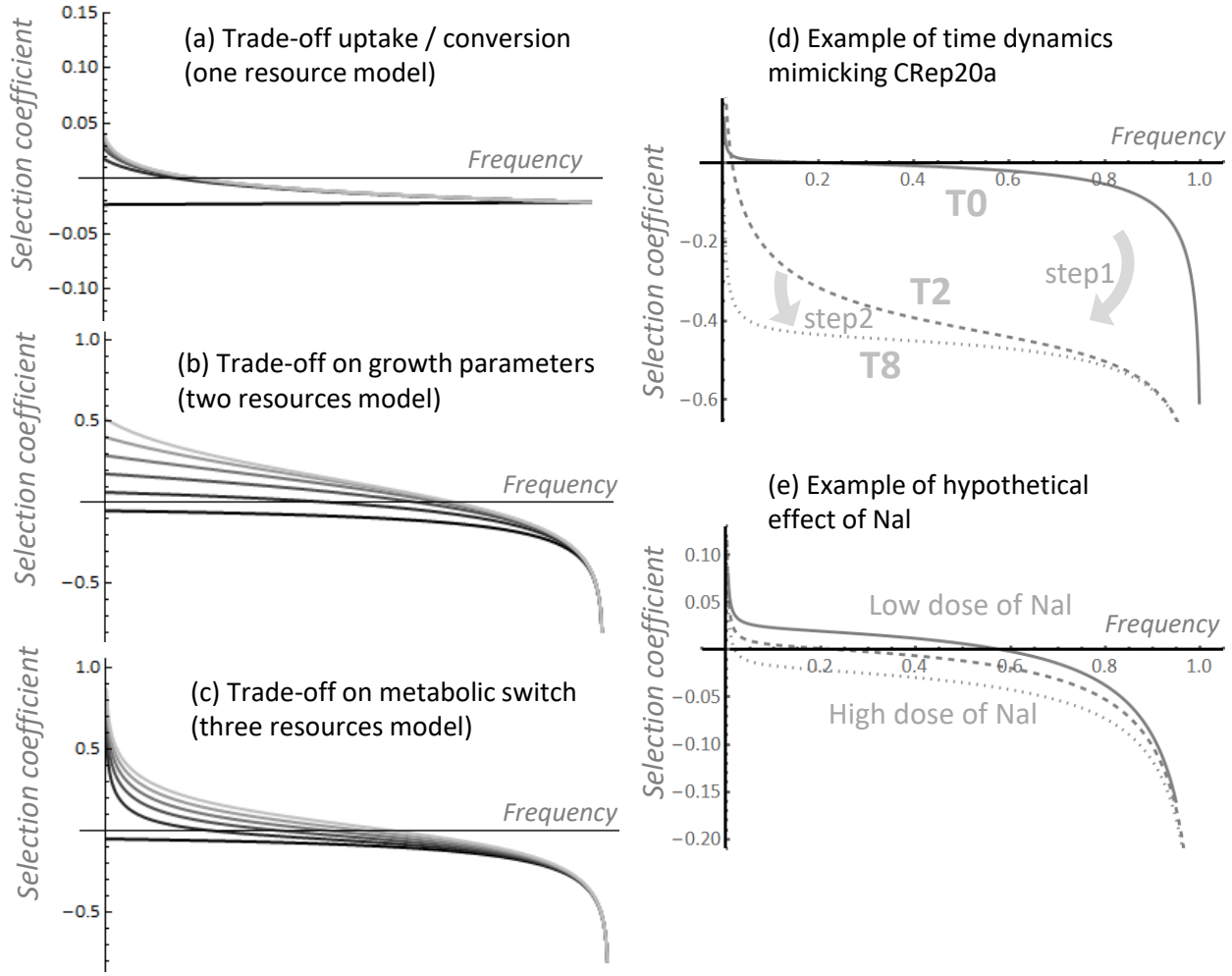
(a) Trade-off uptake / conversion
(one resource model)
Selection coefficient
Frequency
0.15
0.10
0.05
−0.05
−0.10
(b) Trade-off on growth parameters
(two resources model)
Selection coefficient
Frequency
1.0
0.5
−0.5
(c) Trade-off on metabolic switch
(three resources model)
Selection coefficient
Frequency
1.0
0.5
−0.5
(d) Example of time dynamics
mimicking CRep20a
Selection coefficient
Frequency
0.2
0.4
0.6
0.8
1.0
−0.2
−0.4
−0.6
T0
T2
T8
step1
step2
(e) Example of hypothetical
effect of Nal
Selection coefficient
Frequency
0.10
0.05
−0.05
−0.10
−0.15
−0.20
0.2
0.4
0.6
0.8
1.0
Low dose of Nal
High dose of Nal